HHS Public Access

Author manuscript

Methods Enzymol. Author manuscript; available in PMC 2016 January 22.

Published in final edited form as:

Methods Enzymol. 2015 ; 555: 93–125. doi:10.1016/bs.mie.2014.11.022.

Intravital Microscopic Methods to Evaluate Anti-inflammatory Effects and Signaling Mechanisms Evoked by Hydrogen Sulfide

Mozow Y. Zuidema[*] and **Ronald J. Korthuis**[†,‡,1]

[*]Harry S. Truman Veterans Administration Hospital, Cardiology, Columbia, Missouri, USA

[†]Department of Medical Pharmacology and Physiology, School of Medicine, One Hospital Drive, University of Missouri, Columbia, Missouri, USA

[‡]Dalton Cardiovascular Research Center, University of Missouri, Columbia, Missouri, USA

Abstract

Hydrogen sulfide (H_2S) is an endogenous gaseous signaling molecule with potent anti-inflammatory properties. Exogenous application of H_2S donors, administered either acutely during an inflammatory response or as an antecedent preconditioning intervention that invokes the activation of anti-inflammatory cell survival programs, effectively limits leukocyte rolling, adhesion and emigration, generation of reactive oxygen species, chemokine and cell adhesion molecule expression, endothelial barrier disruption,capillary perfusion deficits, and parenchymal cell dysfunction and injury. This chapter focuses on intravital microscopic methods that can be used to assess the anti-inflammatory effects exerted by H_2S, as well as to explore the cellular signaling mechanisms by which this gaseous molecule limits the aforementioned inflammatory responses. Recent advances include use of intravital multiphoton microscopy and optical biosensor technology to explore signaling mechanisms *in vivo*.

1. INTRODUCTION

The cardinal signs of inflammation include vasodilation and increased blood flow, elaboration of proinflammatory mediators, upregulation of adhesion molecule expression on cell surfaces, leukocyte/endothelial cell adhesive interactions, endothelial barrier disruption and edema formation, and tissue injury/dysfunction. In many types of inflammation, generation of reactive oxygen species also occurs and plays important roles in producing many of the other sequelae to an inflammatory stimulus, including parenchymal cell injury. Ischemia and reperfusion (I/R) is now recognized as an inflammatory condition that provokes all of the aforementioned signs of inflammation, but can also be associated with development of capillary perfusion deficits termed the no-reflow phenomenon. Interestingly, capillary no-reflow develops by a neutrophil-dependent mechanism. This chapter focuses on application of intravital microscopic techniques that are used to assess the anti-inflammatory effects of both endogenous H_2S and those invoked by treatment with exogenous H_2S donors, with a particular emphasis on its effects to limit inflammatory responses to I/R.

[1]Corresponding author: korthuisr@health.missouri.edu.

2. MOLECULAR DETERMINANTS OF NEUTROPHIL/ ENDOTHELIAL CELL ADHESIVE INTERACTIONS

The process of neutrophil recruitment to inflammatory sites occurs in 10 distinct phases: margination, capture (tethering) and rolling, slow rolling, arrest (firm adhesion), luminal crawling, transendothelial migration, abluminal crawling, penetration of the basement membrane at regions of low matrix protein deposition and through pericyte gaps, detachment from structures in the vessel wall, and emigration into interstitial tissue (reviewed in Voisin & Nourshargh, 2013; Fig. 1). The adhesion molecules mediating in these steps are different and can vary by leukocyte subset. For the discussion that follows, we focus on adhesive molecules involved in recruiting neutrophils to postischemic tissues, since these cells play the most prominent role in the tissue injury invoked early during reperfusion and our work regarding the anti-adhesive effects of H_2S has focused on that particular question.

Complex and not well-understood hydrodynamic dispersal forces guide neutrophils exiting capillaries to the walls of postcapillary venules, in a process designated as margination. If appropriate adhesive receptors are expressed on both cell types, the neutrophil is initially tethered and begins to roll along the endothelial cell surface. This requires that the adhesive forces tethering leukocytes to the venular surface exceed the shear forces that normally sweep unactivated leukocytes away from quiescent (non-inflammed) endothelial cells. Ischemic vessels exhibit much lower shear rates compared to normally perfused vessels, naturally enhancing the probability for leukocyte–endothelial interactions (Gaboury, Johnston, Niu, & Kubes, 1995; Sanz, Johnston, Issekutz, & Kubes, 1999). Because reperfusion increases the number of rolling and adherent leukocytes and at the same time increases wall shear rate, it is clear that the strength of the adhesive interactions mediating rolling and adhesion are increased relative to nonischemic tissues.

The molecular determinants underlying leukocyte rolling, adhesion and crawling, and transmigration in I/R include specific integrins, members of the immunoglobulin superfamily, and the selectins, as well as a number of other molecular entities expressed on the surfaces of both the infiltrating leukocyte and the endothelium (Voisin & Nourshargh, 2013). These adhesion molecules interact in a highly coordinated and dynamic fashion to allow leukocyte diapedesis into postischemic tissues. E- and P-selectins are expressed on the surface of the endothelium after these cells are activated by proinflammatory mediators formed during I/R. These endothelial selectins interact with L-selectin and PSGL-1 expressed on neutrophils and mediate leukocyte rolling interactions. E-selectin is synthesized de novo, a process which requires 2–4 h, while P-selectin is initially mobilized to the cell surface from a stored pool contained in Weibel–Palade bodies. This is followed by expression of newly synthesized P-selectin 1–4 h later. Thus, endothelial P-selectin participates in leukocyte rolling during early reperfusion while both E- and P-selectin play a role in later periods. During this rolling phase, leukocytes are exposed to and become activated by chemoattractants and intracellular signals. Strengthening of the leukocyte-endothelial interactions occurs primarily through binding of neutrophilic integrin, CD11a/CD18, with its counter-receptor on endothelial cells, ICAM-1 (and perhaps ICAM-2), a

member of the immunoglobulin superfamily. Once arrested, the neutrophil flattens out, which increases the contact area with the endothelium and decreases its cross-sectional profile, allowing it to better resist the effects of shear stress imposed by the flowing blood. The neutrophil then begins to crawl along the endothelial cell by a CD11b/CD18-ICAM-1/ICAM-2-dependent mechanism, often moving against the stream of flowing blood, in search of regions of this barrier that are more amenable to leukocyte diapedesis. Emigration occurs preferentially near tricellular endothelial junctions at sites where ICAM-1 expression is enriched and the underlying basement membrane exhibits low matrix protein deposition. Neutrophils may also exit the circulation by moving directly through endothelial cells, but this occurs much more rarely than egress via intercellular junctions. While mechanisms underlying the former are very unclear, diapedesis via the latter occurs by a process that involves the junctional proteins PECAM-1, ICAM-2, JAM-A, JAM-C, and CD99 interacting with PECAM-1 and CD177, CD11a and CD11b, CD11a, CD11b, CD99, respectively, on neutrophils. Two other endothelial ligands, ESAM and CD99L2, have been shown to play a role in neutrophil migration, but their binding partners on granulocytes are not known. Once the diapedesing neutrophil has penetrated the endothelial barrier, these phagocytic cells crawl along pericytes via CD11a- and CD11b-dependent binding with ICAM-1, interacting with the basement membrane at the same time via VLA-3- and VLA-6-mediated binding to laminins. The abluminally crawling neutrophil breaches these final two barriers by migrating through gaps between pericytes and regions of low matrix protein expression in the basement membrane. Once the neutrophil detaches from these structures in the vessel wall, the cell finally migrates into the interstitial matrix, where chemotactic gradients serve as guidance cues to direct neutrophils to inflammatory loci. For myocardial cells, extravasated neutrophils have been shown interact with ICAM-1, a process that results in increased myocyte ROS levels and cell injury. Oxidant-, platelet activating factor-, leukotriene B_4-, and chemokine-induced leukocyte/endothelial cell interactions are largely responsible for the microvascular dysfunction induced by reperfusion.

3. INTRAVITAL MICROSCOPIC APPROACHES TO STUDY LEUKOCYTE/ENDOTHELIAL CELL ADHESIVE INTERACTIONS

The ability of leukocytes to roll along, adhere (become stationary) to, and transmigrate across microvascular endothelium can be modified by a number of physiologic factors, including adhesion molecule expression on the surface of leukocytes or endothelium, electrostatic charge interactions between surface structures on both cell types, and hydrodynamic dispersal forces which tend to sweep leukocytes along the vessel wall. These adhesive interactions between leukocytes and endothelial cells lining postcapillary venules were first described using transillumination intravital microscopy. By this approach, anesthetized animals are placed on a custom-built animal board, the tissue of interest is surgically exposed and placed over an optically clear viewing pedestal or coverslip mounted over a hole in the animal board, and illuminated from one side using a mercury light source attached to the microscope, with the microscope objective collecting light passing through the tissue and focusing the image on a color camera, which projects the image to a television monitor for data collection (Fig. 2; Ley et al., 2008). However, other preparations that are less mobile because of tissue attachments, such as the rabbit tenuissimus muscle, require

transillumination via a small diameter, curved fiber optic light pipe. The immersion objectives can help prevent motion artifacts while warm superfusate is dripping on the tissue examined. A reducing video coupler (range 0.3 × to 0.6 ×) placed between the camera and the microscope can improve resolution. Suitable tissues, which must be less than 100 μm thick to limit refractive light scattering that would otherwise blur the collected image of the microvessels, include the cremaster muscle or other thin muscles of the rat or mouse, the mesentery of cats, rats, mice, or rabbits, the hamster cheek pouch, or the bat wing (Ley et al., 2008). The dorsal skin-fold chamber represents another approach that allows visualization of a preparation consisting primarily of striated muscle and subcutaneous tissue (Lehr, Vollmar, Vajkoczy, & Menger, 1999). Although surgery is required for chamber implantation, the microcirculation can be observed over extended periods in awake animals, once they recover from implantation. This can also be accomplished using the intact ear of the mouse or the bat wing.

Of the aforementioned models, murine models are now the most popular, given the wide availability of knockout and transgenic mice as well as excellent blocking antibodies that are directed against chemokines and adhesion molecules involved in the various stages of leukocyte–endothelial adhesive interactions. Except for the bat wing and mouse ear, all of the aforementioned preparations are accessible for intravital microscopy only after surgery, which requires anesthesia. It is important to note that choice of anesthetic is important because these agents can differentially influence a number of physiologic processes, including altering sympathetic tone, inducing hormone release, and reducing arterial blood pressure and PO_2. Exposing the bowel requires an abdominal midline incision so that an intestinal loop can exteriorized and draped over the viewing pedestal but no additional dissection to view the mesenteric microcirculation. Nevertheless, bowel exteriorization does some tissue manipulation which can invoke mild to severe inflammatory responses. For example, simply overstretching microvascular vessels or touching the tissue to be observed with surgical instruments, fingers, or moistened cotton swabs as the tissue is manipulated over the viewing pedestal can invoke significant leukocyte interactions with postcapillary venules and/or abolish arteriolar tone. Thus, special care must be taken to minimize tissue manipulation and to avoid touching the area to be viewed. Other preparations, such as the cremaster muscle and other thin muscles, require dissection prior to mounting over coverslip or viewing pedestal. Thus, care must be taken to grasp only the skin overlying the muscles with tweezers prior to making an incision to avoid damage to the underlying muscle tissue. For the cremaster, the connective tissue surrounding the muscle is carefully dissected free without touching the muscle. After pinning one end cremaster so that it lays flat over the viewing coverslip, an incision is made down the center with iris scissors, with care taken to avoid damage to the three main arterial feed vessels and veins. This opens of the saclike structure of the muscle, allowing it to be pinned out for viewing. Microvessels arising from the middle of the three arterial feed vessels are usually selected for study, as they are the farthest removed from the sites of surgical trauma.

In order to minimize inflammation to the tissues being evaluation, the surgical preparation of tissues should be performed with gentle manipulation by skilled surgeons and in a meticulous fashion. Additionally, a sterile environment is imperative to maintain an environment free of bioactive mediators that may interfere with the inflammatory cascade

being studied. Other surgical considerations to maintain physiologic status while isolating the tissue selected for intravital microscopic viewing include intravenous access for anesthesia, intubation for breathing support, blood pressure monitoring, and maintenance of normal central core body temperature with a water-circulating or electrical heating mat and/or thermistor-controlled heat lamps.

Throughout the required surgery and during the remainder of the experimental protocols, the tissue under study must be kept warm (37 for most preparations, 35 °C for the cremaster) and moist in order to obtain physiologically meaningful data (Ley et al., 2008). To accomplish this, the tissue is occasionally rinsed in warmed, buffered physiologic salt solutions during surgery and then continuously superfused with similar solutions once placed over the viewing pedestal or coverslip. Superfusate pO_2 should approximate tissue pO_2 (30 mm Hg for muscle, 40 mm Hg for the mesentery) and pH (7.3–7.4) by bubbling the superfusion reservoir with 95% N_2, 5% CO_2. The tissue can be covered in plastic wrap, which helps in retaining heat and moisture. Because rodents have a large surface area to volume ratio, they lose heat readily, especially when anesthetized, which can dramatically modify physiologic responses. Thus, it is very important to maintain their core temperature 37 °C by use of thermistor-controlled heating pads and/or heating lamps.

When using transillumination intravital microscopy, salt water immersion objectives are used, typically with 20 × magnification and a numerical aperture of 0.5. This provides a wide field of view, encompassing about 300 μm × 400 μm tissue, which allows visualization leukocyte interactions in straight and unbranched portions of venules approximately 15–50 μm in diameter (Ley et al., 2008). Use of immersion objectives allows the tissue to be kept moist and warm by superfusion with physiologic salts solutions, as described above. To provide the greater level of resolution required for examination of the behavior of single adherent and transmigrating leukocytes, higher magnification objectives with larger numerical apertures are employed.

It is important to note that the particular leukocyte subset interacting with the blood vessel wall cannot be identified when using transilluminated intravital microscopy, unless the intravital observations are correlated with histochemical detection of a particular subtype in biopsies obtained at the end of the experiment. Using light microscopy and differential staining of mesenteric samples, nonischemic tissue is sparsely populated by mast cells and leukocytes, with 30–50% of the resident population being neutrophils. On the other hand, I/R produced a significant increase in the number of extravascular leukocytes, with neutrophils constituting greater than 80% of the total cell population. Thus, neutrophils are the predominant leukocyte subtype emigrating from postischemic venules over the time frame of these experiments.

For thicker tissues, such as the mouse intestinal wall, brain, lung, liver, pancreas, Peyer’s patches and peripheral lymph nodes, epifluorescence intravital microscopy is used to visualize leukocyte interactions with the blood vessel wall. Leukocytes can be visualized following intravenous administration of carboxyfluorescein diacetate succinimidyl ester, rhodamine G, or acridine orange, with fluorescent images detected using a charge-coupled device camera. However, this approach again suffers from difficulties in identifying the

leukocyte subset adhering to and emigrating across postcapillary venules. To more specifically visualize neutrophil interactions with the blood vessel walls, some investigators have isolated neutrophils, stained them with fluorescent dyes, and then injected into the experimental animal. This approach can be applied to other specific leukocyte subsets via use of density gradient centrifugation, flow cytometric cell sorting, or magnetic bead selection to isolate a specific type of cell. A problem with this approach is that the isolated, ex vivo labeled neutrophils become activated and behave differently when injected into mice. On the other hand, platelet interactions in the microcirculation can be visualized by this ex vivo isolation/reinjection approach because these thrombocytes are not activated by isolation and ex vivo labeling (Eichorn, Ney, Massberg, & Goetz, 2002; Massberg et al., 1998).

Rather than using nonselective stains, a low dose (3 μg) of neutrophil-specific Alexa-fluor 488 Gr1 antibody is administered intravenously (McDonald et al., 2008, 2010; Peters et al., 2008) to visualize neutrophils in intravital fluorescence microscopy experiments. Alternatively, neutrophils can be specifically visualized by expression of $eGFP^{hi}$ (vs. $eGFP^{low}$ monocytes and macrophages) in LysM-eGFP mice (McDonald et al., 2010; Peters et al., 2008). Several other transgenic and knock-in mice that express green fluorescent protein in only one leukocyte subset (e.g., NKT cells, monocytes, CD4 + or CD8 + T cells) under the control of a subset-specific promotor are also available, which allows adhesive interactions of each subset to be specifically detected and analyzed. Finally, labeling neutrophils with quantum dots conjugated to anti-RP-1 antibody has been employed to visualize these phagocytic cells and their adhesive behaviors in the microcirculation (Jayagopal, Russ, & Haselton, 2007). Care must be taken to illuminate tissues for only brief periods to prevent photobleaching and light toxicity secondary to generation of reactive oxygen species.

Imaging tissues deeper than 100 μm is difficult due to scattering of light, resulting in blurred images. Intravital confocal microscopy greatly improves the resolution and contrast of images in *in vivo* imaging (Jenne, Wong, Petri, & Kubes, 2011; Ley et al., 2008). Use of laser scanning confocal microscopy further enhances the imaging power of intravital microscopy by scanning the laser beam over every point of the focal plane, collecting a stack of sections, and using computer reconstruction algorithms to render a three-dimensional image that can be rotated in all planes. Laser scanning takes too long to apply and collect images and is thus not suitable for leukocyte trafficking studies. However, faster imaging is achieved by use of spinning disk confocal microscopy, which simultaneously detects fluorescence emitted from multiple points and utilizes a charge-coupled device instead of a photomultiplier tube, thereby increasing the rate at which images can be captured (Nakano, 2002). Imaging at greater tissue depths, thinner optical sections, and with decreased photobleaching or phototoxicity can be achieved by use of multiphoton confocal microscopy (Denk & Svoboda, 1997; Ley et al., 2008; Li et al., 2012). Other methods that have been developed to study leukocyte trafficking in deep tissues include single photon emission computed tomography, positron emission tomography, magnetic resonance imaging, and bioluminescence imaging. These methods can noninvasively track leukocytes

over long periods of time, however, they lack the spatial and temporal resolution to visualize single-cell dynamics in situ (Mempel, Scimone, Mora, & von Andrian, 2004).

4. ASSESSING LEUKOCYTE ROLLING, ADHESION, AND EMIGRATION IN THE INTACT MICROCIRCULATION

Leukocyte rolling describes the low affinity adhesive interaction between leukocytes and the vascular endothelium whereby the force of blood flow induces a rotational motion (i.e., rolling) of the leukocyte along the vascular wall. Rolling behavior is most often quantified as the number (or flux) of rolling leukocytes, which is assessed by counting the number of leukocytes flowing past a fixed point (line drawn perpendicular to the long vessel axis on TV monitor) in the vessel of interest that are moving slower than the stream of erythrocytes.

Another way to characterize the behavior of rolling leukocytes is to quantify their velocity (leukocyte rolling velocity, V_{WBC}), determined from the time required for a leukocyte to traverse a given distance along the length of the venule. When expressed relative to the mean erythrocyte velocity (V_{RBC}) in the same vessel, the ratio of V_{WBC}/V_{RBC} provides information regarding the relative strength of the weak adhesive interactions between rolling leukocytes and the endothelium. In other words, V_{WBC}/V_{RBC} provides a measure of the fracture stress at the area of contact between the rolling leukocyte and the endothelium, such that a decrease in V_{WBC}/V_{RBC} indicates a strengthening of this weak adhesive interaction. If the fracture stress increases to a point where it is impossible for adhesive bonds to detach, the leukocyte becomes stationary ($V_{WBC} = 0$), and is defined as a firmly adherent white cell. In practice, an adherent leukocyte is defined as a white cell that remains stationary for 30 s or more, because cells remaining adherent for this length of time then go on to emigrate. Adherent cells are expressed as the number per 100 μm length of venule. Some leukocytes roll along and stop intermittently along the vessel under view and are called saltating leukocytes. The significance of this phenomenon to inflammation is unclear. Emigrated leukocytes are quantified by counting the number of immunocytes outside the blood vessels and are presented as number/field number/mm^2.

Wall shear stress and wall shear rate influence leukocyte rolling and adhesion and thus must be estimated as part of experimental protocols examining leukocyte interactions in microvessels. Wall shear stress (τ) describes the mechanical energy required to peel a leukocyte away from an endothelial cell. Wall shear rate (γ) is defined as the rate at which adjacent layers of fluid move with respect to each other, usually expressed as reciprocal seconds. To obtain estimates of these variables, blood flow centerline velocity is measured. In our laboratory, we use a laser Doppler velocimeter system (Microcirculation Research Institute, Texas A&M University). Microparticle image velocimetry and off-line analysis tools can also be utilizated to assess leukocyte rolling *in vivo*, and can assist in calculating leukocyte rolling flux, leukocyte rolling flux fraction, leukocyte rolling velocity, wall shear rate, and stress and blood flow velocity (Sperandio, Pickard, Unnikrishnan, Acton, & Ley, 2006). Using these velocimetry approaches, venular diameter (D) and centerline red blood cell velocity are measured on-line with a video caliper and an optical Doppler velocimeter, respectively. The velocimeter is calibrated against a rotating glass disc coated with erythrocytes. Venular blood flow is calculated from the product of mean red cell velocity

(V_{mean} = centerline velocity/1.6) (Davis, 1987) and microvascular cross-sectional area, assuming cylindrical geometry.

Wall shear rate (γ) is usually calculated based on the Newtonian definition: $\gamma = 8V_{mean}/D$, where V_{mean} = mean red cell velocity and D = diameter. Wall shear stress (τ) relates viscosity to mean flow velocity and wall shear rate, is calculated from the relation: $\tau = 4V_{mean}\eta/r$, where V = mean blood flow velocity, η = blood viscosity, and r = vessel radius, and is expressed as dyn/cm^2. The number of adherent and extravasated leukocytes and leukocyte rolling velocity are typically determined off-line during playback of videotaped images. Because blood is not a Newtonian fluid, these calculations of γ and τ are, at best, estimates (Ortiz, Briceno, & Cabrales, 2014; Sriram, Intaglietta, & Tartakovsky, 2014), but are useful in determining whether altered shear forces play a role in the changes in leukocyte rolling or adhesion that are invoked by an inflammatory state.

Leukocyte rolling occurs primarily in postcapillary venules and is rarely noted in normal arterioles or capillaries. The numbers of leukocytes rolling along postcapillary venules increases dramatically in inflammatory conditions and is usually associated with an increase in fracture stress (as assessed by decreased V_{WBC}/V_{RBC}). Leukocyte rolling also increases as wall shear rate is reduced below normal, as occurs in ischemic tissues. In normal arterioles, leukocyte adhesion does not occur but a relatively small number of adherent cells have been noted in certain inflammatory conditions, such as treatment with TNFα and in cigarette smoke-exposed animals. Reductions in blood flow and wall shear rate have very little effect on leukocyte adhesion in arterioles.

Recent advances in the use of multicolor fluorescence spinning disk and multiphoton confocal and intravital microscopic imaging has provided important insight regarding the mechanisms whereby neutrophils move abluminally to exit the vascular wall. This work shown that these inflammatory phagocytes migrate along pericytes to exit the vascular wall at regions of low matrix deposition in the basement membrane that are also characterized by gaps between pericytes (Proebstl et al., 2012; Stark et al., 2013; Voisin, Proebstl, & Nourshargh, 2010). Once in the tissue space, neutrophils move through the interstitium by a mechanism dependent on actin polymerization and on matrix metalloproteinase activity but without degradation of pericellular collagen (Lerchenberger et al., 2013).

Because the *in vivo* environment is very complex, unknown or unmeasured variables may influence leukocyte rolling and adhesion. For example, the walls of postcapillary venules are lined by endothelial cells that express a variety of adhesion receptors at different densities which influence leukocyte rolling and adhesion behaviors. As noted above, wall shear rates and the patterns of flow vary with venular diameter, curvature, and branching patterns, which can influence adhesive events in unrecognized ways. In addition, extrinsic factors such as nervous innervation, hormonal inputs, other formed elements in blood (e.g., platelets, other leukocytes, erythrocytes), inflammatory cells resident in the tissue space (e.g., lymphocytes, mast cells), and parenchymal cells all have the potential to influence leukocyte–endothelial interactions. Use of isolated, cannulated postcapillary venules perfused with neutrophils (or other cell types of interest) is an attractive *ex vivo* approach that obviates many of these limitations (Yuan, Mier, Chilian, Zawieja, & Granger, 1995;

Fig. 3). Hence, this approach allows precise evaluation of the direct effects of adhesion molecules and inflammatory mediators in the absence of the complicating effects of these external factors. Moreover, vessels can be perfused with any type of cell that establishes adhesive interactions with postcapillary venular or arteriolar walls, including tumor cells (Kong, Dunn, Keefer, & Korthuis, 1996; Kong & Korthuis, 1997).

As another reductionist approach to study adhesive events under more precisely defined and reproducible conditions, several *in vitro* flow systems have been developed that mimic flow conditions in intact vessels, but can be constructed to eliminate variations in adhesion molecule site density and vascular caliber and orientation that occur *in vivo.* In these systems, microscopic examination of leukocyte interactions with endothelial cells grown on the bottom plate or with specific adhesion molecules or chemokines that are coated onto the plate can be observed and quantified (Ley et al., 2008).

Initial work beginning in the pate 1980s employed parallel plate flow chambers for examination of the effects of shear rate and flow patterns on leukocyte rolling and adhesion. These systems could be perfused with a particular type of leukocyte through the parallel plate with defined geometry, allowing a very accurate assessment of shear rate. This technology underwent several modifications over subsequent years to allow for examination of the role of specific adhesion molecules, expressed either on leukocytes or endothelial cells, in tethering, rolling and adhesion and for examining the molecular mechanisms whereby pro- and anti-adhesive molecules exerted their effects. For example, the plate could be coated with specific adhesion molecules, alone or in various combinations and at varying densities on the plate and leukocyte subsets could be isolated and perfused over these surfaces at different shear rates and flow patterns. However, it soon became apparent that the procedures required to isolate leukocyte subsets altered their activation status, gene expression, and surface expression of adhesion molecules (e.g., L-selectin is shed and CD11b/CD18 is upregulated on neutrophils). To avoid the latter issues, autoperfused flow chamber systems were developed, in which cannula directs blood flowing from the animal through a parallel plate chamber (Ley et al., 2008).

More recently, this autoperfused parallel plate flow chamber approach has been adapted using sophisticated microfluidic technology to fabricate complex microchannel networks (Ley et al., 2008). Because of their small dimensions, these microchannel systems more close mimic the dimensions and flow characteristics in microvessels. In addition, the volume of blood required to perfuse such systems over the course of an experiment is very low, eliminating the requirement for recirculation of the perfusing blood to the donor animal. This obviates concerns related to return of blood containing activating factors that may accumulate during passage through the *in vitro* system. The fact that the microfluidic systems can contain several microchannels allows for high throughput analysis to be conducted. A particularly exciting application of technology is offered by coupling the microfluidic perfusion chamber to total internal reflection microscopy, which allows events at the area of contact between rolling leukocytes and the underyling substrate (Sundd et al., 2012; Sundd, Pospieszakska, & Ley, 2013). While these *in vitro* approaches have not been used to examine the anti-adhesive effects of H_2S, they hold particular promise for study the underlying molecular mechanisms in a highly controlled environment that more accurately

mimics dynamic *in vivo* conditions than traditional static cell culture approaches, while still allowing evaluation of its effects on individual cell types.

5. DETECTION OF CHEMOKINE AND ADHESION MOLECULE EXPRESSION USING INTRAVITAL MICROSCOPY

In addition to monitoring the effects of H_2S or other agents or perturbations on leukocyte rolling, adhesion and emigration in inflammatory states, intravital microscopy can also be applied to the detection of chemokine receptors and expression of adhesion molecules by endothelial cells (Fingar et al., 1997). For example, chemokine receptor expression has been detected by attaching a chemokine such as IL-8 to fluorescent microspheres, which are then injected into the blood stream (Fingar, Taber, et al., 1997). The fluorescent microspheres are 0.1–0.3 μm in diameter, which allows them to readily pass through capillaries, but are large enough to be retained in the circulation and to allow observation and resolution of individual microspheres, once the attached chemokine interacts with its receptor. This allows precise determination of the location of chemokine binding to their specific receptor in the microcirculation, while quantification of fluorescence intensity should provide an estimation of expression levels. A similar approach has been applied to detect ICAM-1 expression on pulmonary endothelial cells using intravital microscopy (Fingar, Guo, Lu, & Peiper, 1997). Sumagin and Sarelius (2010) locally infused an anti-ICAM-1 antibody conjugated to Alexa 388 to detect ICAM-1 expression in postcapillary venules using intravital fluorescence confocal microscopy. Others have employed near infrared light-emitting solid lipid nanoparticles conjugated to ligands specific for integrins to detect expression using intravital microscopy (Shuhendler et al., 2012). Jayagopal et al. (2007) created spectrally distinct quantum dot-antibody bioconjugates directed towards PECAM-1, ICAM-1, and VCAM-1, and following tail vein injection into control and diabetic rats, were able to demonstrate enhanced expression of ICAM-1 and VCAM-1 in large and microcirculatory vessels of the retina, while PECAM-1 fluorescence was similar.

6. INTRAVITAL MICROSCOPIC METHODS TO ASSESS CHANGES IN MICROVASCULAR PERMEABILITY

Increased vascular permeability and edema formation are hallmarks of the inflammatory response. Disruption of endothelial barrier function facilitates blood–tissue exchange of large molecular weight components of the immune response, such as immunoglobulins and complement proteins, at sites of inflammation, thereby enhancing the ability of the immune system to fight infection. In the setting of sterile inflammation, as occurs in ischemic conditions, increased permeability can intensify the deleterious effects of ischemia by promoting edema formation. Excessive accumulation of fluid in the tissue space increases diffusion distance for oxygen and nutrients, exacerbating their already compromised delivery associated with reduced blood supply. In addition, edema raises interstitial fluid pressure, which compresses capillaries thereby contributing to the capillary perfusion deficit referred to as the no-reflow phenomenon. The narrowed capillaries also facilitate leukocyte-capillary plugging to further aggravate this perfusion impairment.

Intravital microscopic methods to assess changes in vascular leakage of large molecules involve administering a fluorescently labeled macromolecule and quantifying the appearance in the extravascular space. Vascular macromolecule leakage does not equate to permeability because it can be increased by enhanced convective transport secondary to elevated microvascular hydrostatic pressure and/or surface area. However, because surface area changes are negligible when observing leakage in single postcapillary venules, vascular macromolecule leakage provides a reasonable index of permeability changes if microvascular hydrostatic pressure changes are measured or if predicted to decrease. To quantify albumin leakage across mesenteric venules, 50 mg/kg of fluorescein isothiacyanate (FITC)-labeled bovine albumin is administered intravenously to the animals 15 min before the baseline recording. Fluorescence intensity is detected with a CCD camera, a CCD camera control unit, and an intensifier head attached to the camera. The fluorescence intensity of the venule under study (I_I), the fluorescence intensity of contiguous perivenular interstitium within 10–50 μm of the venular wall (I_O), and the background fluorescence (I_B) are measured at various times after the administration of FITC-albumin with a computer-assisted digital imaging processor. The windows to measure average fluorescence intensities within and along the venule are set at 20 μm length and 10 μm width. An index of vascular albumin leakage (VAL) is determined from the relation $(I_I - I_B)/(I_O - I_B)$. This method assumes that fluorescent-tagged albumin will move from the microvessel into the tissue space in a manner that reflects the behavior of native albumin.

A more sophisticated application of the same principle underlying the vascular leakage assay relates to assessment of dye accumulation in the interstitial space adjacent to a postcapillary venule that is cannulated with a double bore pipette, with one chamber containing the fluorescent macromolecule of interest (Scallan, Huxley, & Korthuis, 2011). The contents of each chamber in the pipette are under pressure that can control which pipette perfuses the vessel as well as controlling the hydrostatic pressure in the vessel segment. When pipette pressure is adjusted so the dye front is not moving, the pressure measured in the other pipette represents the pressure at the tip and the next downstream bifurcation in the microvascular network. To measure the flux of the labeled solute, pressure is elevated in the pipette to ensure rapid and complete filling of the vessel segment. Recording the step change in fluorescence intensity (I) from perfusion with no labeled solute to perfusion with the tagged macromolecule (I_0)and recording the slope of the tracing depicting the change in intensity as the solute diffuses into the interstitial space ($\Delta I/\Delta t$) allows calculation of permeability of the solute (Ps) from the relation: $(1/I_0)(\Delta I)(\Delta t)(r/2)$, where r = vascular radius and assuming a circular cross-sectional area for the vessel. Using a confocal microscope allows vascular cross-section to be more accurately quantified, providing a better estimate of Ps. The contribution of convective coupling to the flux of the macromolecule can be readily determined by repeating these measurements at a series of hydrostatic pressures. Analysis of the nonlinear relation between solute flux per unit surface area and pressure provides a true measure of diffusive permeability (Pd) that is unaffected by solvent drag (Scallan, Huxley, & Korthuis, 2010).

A measure of water permeability that can be obtained using intravital microscopy involves determination of hydraulic conductivity (Lp) in individually perfused rat mesenteric

postcapillary venules, using the modified Landis technique (Scallan et al., 2010). By this technique, a single postcapillary venule is cannulated with a micropipette and perfused with albumin-ringer solution (control) containing 1% (vol/vol) hamster red blood cells as markers. A known hydrostatic pressure (40–60 cm H_2O), controlled by a water manometer, is applied through the micropipette to the vessel lumen, which allows the perfusate to continuously flow through the vessel. Water flux is measured when the downstream of the vessel is briefly occluded. If intravascular pressures exceed those outside the vessel, fluid filtration occurs and the marker cells will be observed to flow towards the occluder. Just the opposite occurs if intrascular pressures are less than those in the surrounding tissue. Volume flux per unit area (Jv/S) is then calculated from the relation: $(1/x_0)(\Delta x/\Delta t)(r/2)$; where Δx is the distance the marker cell moves over an interval of time (Δt), having started at distance x_0, and r = vessel radius. When these measures are repeated at several pressures, the slope of the line relating Jv/S to pressure is equal to Lp. The intercept of such a plot yields the effective osmotic pressure gradient.

As noted above, the inflammatory milieu is characterized by a large number of factors extrinsic to the vascular wall of postcapillary walls that influence leukocyte–endothelial cell interactions. These same factors also influence venular permeability responses, necessitating the development of approaches that allow precise control of these external factors, so that their individual contributions to barrier disruption can be assessed. Isolated, perfused postcapillary venules have proven useful in this regard (Breslin et al., 2006; Yuan, Chilian, Granger, & Zawieja, 1993; Fig. 3). Cell culture models, especially those involving endothelial cells grown on top of a three-dimensional extracellular matrix that can be seeded with inflammatory cells of interest should prove invaluable, especially in models that incorporate shear stress exposure.

7. ASSESSMENT OF REACTIVE OXYGEN SPECIES GENERATION USING INTRAVITAL MICROSCOPY

The production of ROS in the microvasculature can be determined by monitoring the oxidation of dihydrorhodamine (DHR) to its fluorphore rhodamine 123, using intravital digital microfluorography. To make this measurement, long segments (300 μm) of postcapillary venules are identified and selected for viewing using intravital microscopy. Background fluorescence (I_{Bgrd}) of the first 100 μm of each 300-μm vessel length is recorded from the selected postcapillary venules with a xenon light source and a SIT camera system. Then, freshly prepared DHR-123 (1 mmol/L, a nonfluorescent dye that is oxidized by ROS to the fluorescent compound rhodamine-123) in bicarbonate-buffered saline is superfused over the tissue being observed for 15 min. The tissue is then washed with bicarbonate-buffered saline and the fluorescent image of each vessel section recorded (I_{DHR}). Images are captured onto a computer, and an area 100 μm long and 7 μm wide along the vessel wall is analyzed in each vascular segment using imaging software. The ratio of I_{DHR}:I_{Bgrd} is calculated for each vascular segment, and the average ratio for each animal determined. Although some have claimed that DHR oxidation may be specific detector for peroxynitrite, subsequent work indicated that it interacts with many radical species and peroxidases.

Dichlorofluorescein (DCFH) diacetate is another oxidant-sensitive probe that has been used in intravital microscopic studies to detect ROS production in the intact microcirculation (Suematsu et al., 1993). DCFH diacetate diffuses into cells in a nonfluorescent form that is cleaved by esterases to DCFH, which is trapped intracellularly. Exposure to hydroperoxides as they are formed in cells oxidizes DCFH to yield fluorescent dihydrofluorescein (DCF). After obtaining a background autofluorescence image, the fluorochrome is added to the superfusate bathing the tissue at a concentration of 5 μM and perfused over the tissue under observation for 25 min, followed by 10 min rinse with DCFH diacetate-free superfusate to remove the dye precursor from the tissue. Fluorescence is detected using epifluorescence microscopy and quantified using image analysis software (Suematsu et al., 1993, 1994).

These techniques not only allowed for oxidant detection but also their topographic distribution in microcirculatory units. However, it is important to point out that data obtained using oxidant-sensitive probes *in vivo* are widely misinterpreted with regard to their ability to indicate specific types of reactive oxygen species that are being generated (Grisham, 2013; Winterbourn, 2014). Thus, while data obtained with DCFH diacetate or DHR dye detection approaches are often interpreted to be indicative of hydrogen peroxide production, these indicators react with a number of oxidizing species. Similarly, hydroethidine has been used as a superoxidespecific detector in intravital microscopic studies (Suzuki et al., 1998), but is also now recognized to be oxidized nonspecifically by a mechanism similar to DCFH (Winterbourn, 2014). Thus, oxidant-sensitive probes are useful for detecting ROS in tissues viewed by intravital microscopy, but conclusions based on this data should not be extrapolated to specific radical species. The recent development of genetically encoded ROS reporters and nanoparticle dye delivery systems may be useful in this regard, but have not yet been optimized for application in studies using intravital microscopy (Ezerina, Morgan, & Dick, 2014; Morgan, Sobotta, & Dick, 2011; Woolley, Stanicka, & Cotter, 2013).

8. FLUORESCENCE DETECTION OF CELL INJURY USING INTRAVITAL MICROSCOPY

Cell injury can be quantified in tissues using vital dyes. Propidium iodide (PI) and ethidium bromide have both been shown to be effective indicators of tissue injury and can be quantified using intravital microscopy (Dungey et al., 2006; Harris, Costa, Delano, Zweifach, & Schmid-Schonbein, 1998; Harris, Leiderer, Peer, & Messmer, 1996; Suematsu et al., 1994). PI is a positively charged indicator dye that is unable to cross cell membranes. However, when cells are injured an unable to maintain membrane potential difference across the plasmalemma, PI enters cells, binds to nuclear DNA, and becomes fluorescent. PI is either injected intravenously at a dose of 1 μ*M*/kg body weight or can be superfused over the tissue at a concentration of 1 μ*M* and the number of PI-positive cells in the field of view are counted as a measure of nonviable cells. As another approach, the fluorescent vital dyes bisbenzimide, which stains the nuclei of all cells, and the larger ethidium bromide molecule, which can only enter cells whose membranes have been injured, can be used. Ethidium bromide labels the nuclei of cells with a range of injury from minor (membrane permeable) to death. Ethidium bromide (5 μg/mL) and bisbenzimide (5 μg/mL) are added to the

superfusate, and cell injury measured by recording fluorescent illumination with the appropriate filters for the two indicators, with injury expressed as a ratio cells stained with ethidium bromide to bisbenzimide-positive cells.

9. PERFUSED CAPILLARY DENSITY ASSESSMENT WITH INTRAVITAL MICROSCOPY

I/R causes the development of a capillary perfusion impairment called the no-reflow phenomenon. The extent of no-reflow can be readily assessed using intravital microscopy by counting the number of capillaries crossing perpendicular to a line drawn on the television monitor onto which the microvascular field is projected that exhibit flowing erythrocytes under control conditions or following I/R (Dungey et al., 2006). Others have quantified functional capillary density by measuring the length of capillaries perfused with red blood cells per observation area (Harris et al., 1996).

10. ACUTE AND PRECONDITIONING-INDUCED ANTI-INFLAMMATORY ACTIONS OF HYDROGEN SULFIDE: ASSESSMENT USING INTRAVITAL MICROSCOPY

Although once only regarded as a toxic gas, hydrogen sulfide (H_2S) was recently identified as an endogenously produced signaling molecule that exerts effects at the molecular, cellular, tissue, and system levels (Abe & Kimura, 1996; Kamoun, 2004; Kashiba, Kajimura, Godo, & Suematsu, 2002; Wang, 2003, 2012). Hydrogen sulfide and its major dissociation product, HS^-, are extremely reactive, most likely exerting biological effects through direct covalent modification of target molecules. On the one hand, HS^- is a potent chemical reductant and nucleophile that allows it to scavenge free radicals by single electron or hydrogen atom transfer, while on the other H_2S is a thiol and can interact with and “scavenge” free radicals (Wang, 2012).

H_2S is produced endogenously by the actions of cystathionine-β-synthase (CBS) or cystathionine-γ-lyase (CSE), which use cysteine or homocysteine as substrate. Another enzyme, 3-mercaptopyruvate sulfurtransferase, working in concert with cysteine aminotransferase, can metabolize cysteine to generate pyruvate and H_2S. These enzymes are differentially expressed across tissues and organs of the body, with CSE being the predominant H_2S-generating enzyme in both vascular smooth muscle and endothelial cells (Wang, 2012). Like the other gaseous signaling molecules (nitric oxide, carbon monoxide, ammonia, and perhaps methane). H_2S is a small molecule that easily traverses cell membranes, has a short half-life, and is synthesized on demand.

Use of intravital microscopy has proven to be an invaluable tool in evaluating the role of endogenously produced H_2S and hydrogen sulfide donors on leukocyte–endothelial cell adhesive interactions. Zanardo et al. (2006) were amongst the first to demonstrate that pharmacologic CSE inhibition produced a decrease in leukocyte rolling velocity and increased stationary adherence relative to control rats under baseline conditions. On the other hand, CSE inhibition enhanced carrageenan-induced leukocyte infiltration in an air

pouch inflammatory model. These observations were interpreted to indicate that H_2S facilitates the presentation of a nonadhesive endothelial surface under baseline conditions and that endogenous production of this gaseous signaling molecule is an important modulator of acute inflammation. In this same study, pretreatment with the H_2S donors, NaHS, Na_2S, or Lawesson's reagent, markedly reduced the enhanced rolling and adhesive responses noted in mesenteric postcapillary venules that were induced by intragastric aspirin or superfusion with proinflammatory fMLP. Similar observations were made in mice heterozygous for the CBS gene expression, which should reduce the bioavailability of H_2S, and fed a hyperhomocysteinemic diet. The mutant mice demonstrated marked reductions in leukocyte rolling velocity and increased stationary adhesion relative to wild-type (WT) mice fed the same diet (Kamath et al., 2006). Intravital microscopy has also been used to quantify the effects of H_2S to limit the extent of capillary no-reflow in the kidney and hepatic sinusoidal leukocyte rolling and adhesion induced by renal ischemia/reperfusion (Zhu et al., 2012). Protective effects of H_2S donor treatment on neurovascular permeability induced by hyperhomocysteinemia and leukocyte trafficking in inflamed joints have also been reported (Andruski, McCafferty, Ignacy, Millen, & McDougall, 2008; Tyagi et al., 2010). H_2S also limits leukocyte adherence to vascular endothelium provoked by exposure to nonsteroidal anti-inflammatory drugs (Fiorucci et al., 2005; Zanardo et al., 2006).

The molecular signaling mechanisms invoked by H_2S to limit baseline or proinflammatory mediator-induced leukocyte rolling and adhesion are only now becoming apparent. It appears that ATP-sensitive potassium (K_{ATP}) channel activation by H_2S may be important, because its anti-adhesive and -inflammatory effects were blocked by coincident treatment with a pharmacologic K_{ATP} channel inhibitor (Zanardo et al., 2006). Preliminary work supports a role for neutrophilic annexin A1 (AnxA1) in the antiadhesive effects of H_2S donor treatment (Brancaleone, Flower, Cirino, & Perretti, 2013). In this study, the ability of H_2S donor treatment to limit interleukin-1β-induced leukocyte adhesion noted in WT mice was not apparent in AnxA1 knockout mice. Moreover, treatment of human neutrophils with the same donor, produced a marked mobilization of AnxA1 to the cell surface. Interestingly, fluorescent beads coated with an antibody to P-selectin adhered in much greater numbers when infused into heterozygous CBS +/−mice compared to WT animals. The latter result supports the possibility that P-selectin expression could be an important end-effector target in the anti-adhesive effects of endogenous H_2S. From these isolated observations, it is not clear whether what signaling steps are invoked by H_2S to activate K_{ATP} channels or cause mobilization of AnxA1, or whether these two signaling elements are mechanistically linked in the same cell type or to endothelial P-selectin expression. These potential linkages could be readily addressed by intravital microscopic studies involving WT and chimeric mice.

In contrast to the aforementioned anti-adhesive effects of endogenous and exogenous H_2S, this signaling molecule appears to enhance leukocyte rolling and adhesion in mesenteric venules in a cecal ligation and puncture (CLP) sepsis model (Zhang, Zhi, Moochhala, Moore, & Bhatia, 2007). In these studies, treatment with an inhibitor of H_2S formation significantly reduced the numbers of rolling and firmly adherent leukocytes and increased leukocyte rolling velocity in septic mice. On the other hand, septic mice treated with an H_2S donor at the time of sepsis induction exhibited enhanced increases in leukocyte rolling and adherence. These changes were linked to an effect of H_2S to enhance adhesion molecule

expression in septic mice. In stark contrast to the aforementioned results, Spiller et al. (2010) showed that H_2S donor treatment reduced mesenteric leukocyte rolling and adhesion in CLP sepsis. It is not clear what accounts for these divergent responses but could be due to differences in sepsis severity in the two studies.

In addition to these acute effects of H_2S treatment, a growing body of evidence indicates that antecedent preconditioning with H_2S donors elicits the development of an anti-inflammatory phenotype in tissues that are exposed to I/R 24 h later. Preconditioning refers to a phenomenon where antecedent exposure to a particular stimulus confers protection against the deleterious effects induced by subsequent exposure to prolonged I/R (Krenz, Baines, Kalogeris, & Korthuis, 2013). Preconditioning stimuli typically produce two phases of protection in I/R. Acute or early phase preconditioning develops rapidly (within minutes), involves activation of pre-existing effector molecules, and is short-lived, conferring protection for 2–6 h before disappearing. Delayed acquisition of tolerance to ischemia (late phase preconditioning) arises 12–24 h after the initial preconditioning stimulus is applied, is longer lived (24 h or longer), and requires expression of new gene products to mediate protection (Krenz et al., 2013).

The observations that H_2S donors produce vasodilation by activation of K_{ATP} channels and enhances the vasorelaxant effects of NO (Wang, 2003, 2012), coupled with the fact that K_{ATP} channel activators and NO donors elicit preconditioning (Krenz et al., 2013), led us to postulate that this gaseous signaling molecule could also serve as a preconditioning stimulus to limit the proinflammatory effects of I/R (Yusof, Kamada, Kalogeris, Gaskin, & Korthuis, 2009). To address this issue, we first sought to determine whether and H_2S donor (NaHS) preconditioning would elicit anti-inflammatory effects in tissues exposed to I/R one (acute preconditioning) or 24 h (delayed preconditioning) after NaHS treatment. Only delayed H_2S preconditioning caused postcapillary venules to shift to an anti-inflammatory phenotype in WT mice after I/R such that these vessels failed to support leukocyte rolling and adhesion during reperfusion. To our knowledge, this is the only pharmacologic preconditioning agent that produces late but not early phase preconditioning, suggesting that H_2S may induce preconditioning by mechanisms that have signaling elements distinct from other approaches.

The protective effect of delayed NaHS preconditioning to decrease postischemic leukocyte rolling was largely abolished by coincident NO synthase (NOS) inhibition in WT mice and was absent in eNOS knockout mice (Yusof et al., 2009). A similar pattern of response was noted for leukocyte rolling in WT mice treated with NaHS concomitant with p38 MAPK inhibitors. The effect of late phase NaHS preconditioning on stationary (firm) leukocyte adhesion was also attenuated by treatment with NOS and p38 MAPK inhibitors in WT mice, but the anti-adhesive effect of NaHS was still evident in eNOS-deficient mice. These studies indicate that delayed NaHS preconditioning prevents postischemic leukocyte rolling and adhesion by triggering activation of an eNOS- and p38 MAPK-dependent mechanism. However, the role of eNOS in the anti-adhesive effect of NaHS preconditioning was less prominent than its effect to reduce leukocyte rolling. In subsequent work, we demonstrated that large conductance, calcium-activated potassium (BKCa) channels (but not small (SKCa) or intermediate (IKCa) conductance, calcium-activated potassium channels) also play an important role in triggering or initiating the anti-adhesive effects of NaHS preconditioning

that become manifest during I/R 24 h later (Zuidema et al., 2010). We have also obtained evidence implicating a role for activation of plasmalemmal (pK_{ATP}) and mitochondrial K_{ATP} ($mitoK_{ATP}$) channels as initiators of NaHS preconditioning (Zuidema, Gross, & Korthuis, unpublished observations). As we have also shown that NaHS preconditioning, activation of BKCa channels, or neutrophil depletion were also effective in preventing mucosal mitochondrial dysfunction induced by I/R (Liu et al., 2012), it is clear that the effect of antecedent H_2S donor treatment to limit postischemic leukocyte/endothelial interactions ultimately acts to attenuate tissue injury in I/R by preventing trafficking of neutrophils.

While the aforementioned studies clearly established roles for eNOS-derived NO, phosphorylation of p38 MAPK, and activation of pK_{ATP}, $mitoK_{ATP}$, and BKCa channels as essential triggers to inaugurate entrance into a preconditioned anti-inflammatory phenotype by antecedent NaHS (Fig. 4), the molecular entities responsible for mediating that ability of postcapillary venules to resist supporting leukocyte rolling and adhesion during I/R were unknown. Since the reaction products of heme oxygenase-1 (HO-1)-mediated heme degradation exhibit powerful anti-adhesive and antioxidant properties, we postulated that this stress protein might serve this effector function in NaHS preconditioning (Zuidema, Peyton, Fay, Durante, & Korthuis, 2011). We showed that NaHS produced an increase in HO-1 expression at 8 and 24 h after administration, but not at earlier time points. HO activity in tissues samples was also elevated, when assessed 24 h after NaHS treatment. Moreover, pharmacologic HO inhibition during reperfusion prevented the ability of antecedent NaHS to abolish postischemic leukocyte rolling and adhesion in WT animals. NaHS preconditioning was also ineffective in mice genetically deficient in HO-1. These data indicate that HO-1 serves as an important end-effector of the anti-adhesive cytoprotective effects of antecedent H_2S treatment.

Taken together, the aforementioned late phase NaHS preconditioning studies support the view that H_2S initiates entrance into a preconditioned state by an eNOS-derived NO-, p38 MAPK-, BKCa channel-, and K_{ATP} channel-dependent mechanism to invoke increased expression and activity of HO-1 24 h later (Fig. 4). HO-1-catalyzed formation of carbon monoxide, bilirubin, and secondarily derived biliverdin act to limit postischemic leukocyte rolling and adhesion by preventing adhesion molecule expression and scavenging ROS as they are produced.

11. CONCLUSION AND PERSPECTIVES

Use of intravital microscopic approaches to study the effects of endogenously produced H_2S on postcapillary venular function have clearly established that baseline production of the gaseous signaling molecule, most likely by endothelial cells but perhaps also by the underlying pericyte layer, downregulates endothelial adhesion molecule expression to maintain a non-adhesive surface. Moreover, it is clear that use of exogenous H_2S donors exert powerful and direct anti-adhesive effects in inflamed tissues that target the expression of adhesion molecules to limit leukocyte–endothelial cell adhesive interactions. Although surprisingly little research has been directed at uncovering the anti-inflammatory mechanisms that are invoked by the acute administration of H_2S donors during

inflammation, we have begun to uncover the signaling pathways invoked by preconditioning tissues with H_2S donors 24 h prior to I/R. Because of potential off-target or even deleterious effects of H_2S (e.g., poisoning mitochondrial respiratory chain by binding to the iron of cytochrome c oxygenase), uncovering the signaling mechanisms that underlie the anti-inflammatory effects of H_2S donors may lead to the development of novel therapies to treat conditions characterized by increased leukocyte–endothelial interactions. Promising new directions in this regard relate to use of BKCa activators or inducers of HO-1. Other promising developments with regard to pharmacologic development relate to development of analogues that modify the rate and amount of H_2S release from donor molecules or allow their administration via routes (inhalation, injection, skin patch, oral intake) that enhance patient compliance and/or treatment efficacy when these compounds enter human trials. Other strategies that may enhance translational therapeutics include formulation of H_2S-releasing nonsteroidal anti-inflammatory drugs (NSAIDs) as an approach to reduce gastrointestinal bleeding and ulceration that often accompanies chronic use of NSAIDS in arthritic patients (Fiorucci et al., 2005; Wallace et al., 2014; Zanardo et al., 2006). H_2S-releasing derivatives of other drugs, such as mesalamine, have also been developed to improve their anti-inflammatory potency and effectiveness (Fiorucci et al., 2007).

The power of intravital microscopy for the assessment of inflammatory responses and their modulation by H_2S donors in the intact living microcirculation has not been fully utilized. Nearly all studies have concentrated on effects of these agents on leukocyte rolling and adhesion, with very few or no studies focusing on platelet adhesion, chemokine and adhesion molecule expression, venular permeability, generation of ROS and RNOS, perfused capillary density, or cellular injury via use of techniques described above. As a consequence, the field has relied on *in vitro* and or *ex vivo* approaches to obtain much of what is known about the effect of H_2S donors on changes in chemokine and adhesion molecule expression, venular permeability, ROS/RNOS generation, and cellular injury induced by proinflammatory stimuli. Certainly, important new information has arisen from these *in vitro* approaches and immunohistochemical data obtained from tissue sections regarding the mechanisms underlying the anti-inflammatory effects of H_2S. However, these results do not necessarily inform us about the relative contributions of these mechanisms in the living microcirculation. Indeed, the unanticipated complexity of the *in vivo* milieu is often cited as a major contributing factor to the very high percentage (>93%) of failed clinical trials related to new cardiovascular (and other) drugs. Comparing the effects of H_2S on these variables in the more complicated *in vivo* milieu to data obtained from *in vitro* systems allows assessment of which of the many possibilities defined in vitro actually occur in the living microcirculation.

One new area for application of intravital microscopy that may significantly enhance the power of *in vivo* approaches to study mechanisms at the cell and molecular level relates to the development of novel approaches to visualize and quantify signal transduction events in intact vessels and microvascular networks of the living animal. As an example, Tallini et al. (2007) genetically engineered transgenic mice to study endothelial cell-specific calcium signaling *in vivo*. In these mice, the Ca^{2+} sensor GCaMP2 was placed under the control connexin 40 transcription regulatory elements within a bacterial artificial chromosome, a

transgenesis approach that produces a mouse with endothelium lineage-specific calcium signaling. Using these mice, these investigators showed that bidirectional conduction of vasodilation mediated by relaxation of vascular smooth muscle cells along arteriolar networks involves a wave of Ca^{2+} that travels along the endothelium. Mauban, Fairfax, Rizzo, Zhang, and Wier (2014) used the GCaMP2 approach and a FRET-based genetically encoded Ca^{2+}/calmodulin sensor biomolecule (exMLCK) indicator, combined with two-photon fluorescence microscopy, to noninvasively quantify vascular smooth muscle Ca^{2+} in specific vessels in the ear of unanesthetized mice over extended periods of time as hypertension developed (Mauban et al., 2014). Continued development of new FRET-based optical biosensors that target other signaling molecules, coupled with spinning disk confocal or multiphoton imaging, would allow us to learn exactly what cells, and where in those cells, the molecule of interest was being activated in the living microcirculation. In addition to these approaches, use of immunocytes derived from GFP and YFP mice that are adoptively immunotransferred into wild type mice will facilitate the study of cell–cell interactions in signaling inflammatory responses and how this intercellular communication is influenced by H_2S donor treatment.

ACKNOWLEDGMENT

This work was supported by a grant from the National Institutes of Health (PO1 HL095486).

REFERENCES

Abe K, Kimura H. The possible role of hydrogen sulfide as an endogenous neuromodulator. Journal of Neuroscience. 1996; 16(3):1066–1071. [PubMed: 8558235]

Andruski B, McCafferty DM, Ignacy T, Millen B, McDougall JJ. Leu-kocyte trafficking and pain behavioral responses to a hydrogen sulfide donor in acute monoarthritis. American Journal of Physiology. Regulatory, Integrative and Comparative Physiology. 2008; 295(3):R814–R820.

Brancaleone V, Flower RJ, Cirino G, Perretti M. OP06 annexin A1 (AnxA1) mediates hydrogen sulfide (H2S) effects in the control of inflammation. Nitric Oxide. 2013; S1–31(Suppl. 2):S21–S22.

Breslin JW, Sun H, Xu W, Rodarte C, Moy AB, Wu MH, et al. Involvement of ROCK-mediated endothelial tension development in neutrophil-stimulated microvascular leakage. American Journal of Physiology. Heart and Circulatory Physiology. 2006; 290(2):H741–H750. [PubMed: 16172166]

Davis MJ. Determination of volumetric flow in capillary tubes using an optical Doppler velocimeter. Microvascular Research. 1987; 34:223–230. [PubMed: 2959844]

Denk W, Svoboda K. Photon upmanship: Why multiphoton imaging is more than a gimmick. Neuron. 1997; 18(3):351–357. [PubMed: 9115730]

Dungey AA, Badhwar A, Bihari A, Kvietys PR, Harris KA, Forbes TL, et al. Role of heme oxygenase in the protection afforded skeletal muscle during ischemic tolerance. Microcirculation. 2006; 13(2): 71–79. [PubMed: 16459320]

Eichorn ME, Ney L, Massberg S, Goetz AE. Platelet kinetics in the pulmonary microcirculation *in vivo* assessed by intravital microscopy. Journal of Vascular Research. 2002; 39:330–339. [PubMed: 12187123]

Ezerina D, Morgan B, Dick TP. Imaging dynamic redox processes with genetically encoded probes. Journal of Molecular and Cellular Cardiology. 2014; 73:43–49. [PubMed: 24406687]

Fingar VH, Guo HH, Lu ZH, Peiper SC. Expression of chemokine receptors by endothelial cells: Detection by intravital microscopy using chemokine-coated fluorescent microspheres. Methods in Enzymology. 1997; 288:148–158. [PubMed: 9356993]

Fingar VH, Taber SW, Buschemeyer WC, ten Tije A, Cerrito PB, Tseng M, et al. Constitutive and stimulated expression of ICAM-1 protein on pulmonary endothelial cells *in vivo*. Microvascular Research. 1997; 54(2):135–144. [PubMed: 9327384]

Fiorucci S, Antonelli E, Distrutti E, Rizzo G, Mencarelli A, Orlandi S, et al. Inhibition of hydrogen sulfide generation contributes to gastric injury caused by anti-inflammatory nonsteroidal drugs. Gastroenterology. 2005; 129(4):1210–1224. [PubMed: 16230075]

Fiorucci S, Orlandi S, Mencarelli A, Caliendo G, Santagada V, Distrutti E, et al. Enhanced activity of a hydrogen sulphide-releasing derivative of mesalamine (ATB-429) in a mouse model of colitis. British Journal of Pharmacology. 2007; 150(8):996–1002. [PubMed: 17339831]

Gaboury JP, Johnston B, Niu XF, Kubes P. Mechanisms underlying acute mast cell-induced leukocyte rolling and adhesion *in vivo*. Journal of Immunology. 1995; 154(2):804–813.

Grisham MB. Methods to detect hydrogen peroxide in living cells: Possibilities and pitfalls. Comparative Biochemistry and Physiology. Part A, Molecular & Integrative Physiology. 2013; 165(4):429–438.

Harris AG, Costa JJ, Delano FA, Zweifach BW, Schmid-Schonbein GW. Mechanisms of cell injury in rat mesentery and cremaster muscle. American Journal of Physiology. 1998; 274(3):H1009–H1015. Pt 2. [PubMed: 9530215]

Harris AG, Leiderer R, Peer F, Messmer K. Skeletal muscle microvascular and tissue injury after varying durations of ischemia. American Journal of Physiology. 1996; 271(6):H2388–H2398. Pt 2. [PubMed: 8997297]

Jayagopal A, Russ PK, Haselton FR. Surface engineering of quantum dots for *in vivo* vascular imaging. Bioconjugate Chemistry. 2007; 18(5):1424–1433. [PubMed: 17760416]

Jenne CN, Wong CH, Petri B, Kubes P. The use of spinning-disk confocal microscopy for the intravital analysis of platelet dynamics in response to systemic and local inflammation. PLoS One. 2011; 6(9):e25109. [PubMed: 21949865]

Kamath AF, Chauhan AK, Kisucka J, Dole VS, Loscalzo J, Handy DE, et al. Elevated levels of homocysteine compromise blood-brain barrier integrity in mice. Blood. 2006; 107(2):591–593. [PubMed: 16189268]

Kamoun P. Endogenous production of hydrogen sulfide in mammals. Amino Acids. 2004; 26(3):243–254. [PubMed: 15221504]

Kashiba M, Kajimura M, Godo N, Suematsu M. From O_2 to H_2S: A landscape view of gas biology. Keio Journal of Medicine. 2002; 51(1):1–10. [PubMed: 11951372]

Kong L, Dunn GD, Keefer LK, Korthuis RJ. Nitric oxide reduces tumor cell adhesion to isolated rat postcapillary venules. Clinical & Experimental Metastasis. 1996; 14(4):335–343. [PubMed: 8878407]

Kong L, Korthuis RJ. Melanoma cell adhesion to injured arterioles: Mechanisms of stabilized tethering. Clinical & Experimental Metastasis. 1997; 15(4):426–431. [PubMed: 9219731]

Krenz, M.; Baines, C.; Kalogeris, T.; Korthuis, RJ. Cell survival programs and ischemia/reperfusion: Hormesis, preconditioning, and cardioprotection. In: Granger, DN.; Granger, J., editors. Colloquium series on integrated systems physiology: From molecule to function to disease. Morgan and Claypool; San Rafael, CA: 2013.

Lehr HA, Vollmar B, Vajkoczy P, Menger MD. Intravital fluorescence microscopy for the study of leukocyte interaction with platelets and endothelial cells. Methods in Enzymology. 1999; 300:462–481. [PubMed: 9919547]

Lerchenberger M, Uhl B, Stark K, Zuchtriegel G, Eckart A, Miller J, et al. Matrix metalloproteinases modulate ameoboid-like migration of neutrophils through inflamed interstitial tissue. Blood. 2013; 122:770–780. [PubMed: 23757732]

Ley K, Mestas J, Pospieszalska MK, Sundd P, Groisman A, Zarbock A. Chapter 11. Intravital microscopic investigation of leukocyte interactions with the blood vessel wall. Methods in Enzymology. 2008; 445:255–279.http://dx.doi.org/10.1016/S0076-6879(08)03011-5 [PubMed: 19022063]

Li W, Nava RG, Bribriesco AC, Zinselmeyer BH, Spahn JH, Gelman AE, et al. Intravital 2-photon imaging of leukocyte trafficking in beating heart. Journal of Clinical Investigation. 2012; 122(7): 2499–2508. [PubMed: 22706307]

Liu Y, Kalogeris T, Wang M, Zuidema MY, Wang Q, Dai H, et al. Hydrogen sulfide preconditioning or neutrophil depletion attenuates ischemia-reperfusion-induced mitochondrial dysfunction in rat

small intestine. American Journal of Physiology. Gastrointestinal and Liver Physiology. 2012; 302(1):G44–G54. [PubMed: 21921289]

Massberg S, Enders G, Leiderer R, Eisenmenger S, Vestweber D, Krombach F, et al. Platelet-endothelial cell interactions during ischemia/reperfusion: The role of P-selectin. Blood. 1998; 92:507–515. [PubMed: 9657750]

Mauban JR, Fairfax ST, Rizzo MA, Zhang J, Wier WG. A method for noninvasive longitudinal measurements of [Ca2 +] in arterioles of hypertensive optical biosensor mice. American Journal of Physiology. Heart and Circulatory Physiology. 2014; 307(2):H173–H181. [PubMed: 24858846]

McDonald B, McAvoy EF, Lam F, Gill V, de la Motte C, Savani RC, et al. Interaction of CD44 and hyaluronan is the dominant mechanism for neutrophil sequestration in inflamed liver sinusoids. Journal of Experimental Medicine. 2008; 205(4):915–927. [PubMed: 18362172]

McDonald B, Pittman K, Menezes GB, Hirota SA, Slaba I, Waterhouse CC, et al. Intravascular danger signals guide neutrophils to sites of sterile inflammation. Science. 2010; 330(6002):362–366. [PubMed: 20947763]

Mempel TR, Scimone ML, Mora JR, von Andrian UH. *in vivo* imaging of leukocyte trafficking in blood vessels and tissues. Current Opinion in Immunology. 2004; 16(4):406–417.http://dx.doi.org/10.1016/j.coi.2004.05.018 [PubMed: 15245733]

Morgan B, Sobotta MC, Dick TP. Measuring E(GSH) and H2O2 with roGFP2-based redox probes. Free Radical Biology and Medicine. 2011; 51(11):1943–1951. [PubMed: 21964034]

Nakano A. Spinning-disk confocal microscopy—A cutting-edge tool for imaging of membrane traffic. Cell Structure and Function. 2002; 27(5):349–355. [PubMed: 12502889]

Ortiz D, Briceno JC, Cabrales P. Microhemodynamic parameters quantification from intravital microscopy videos. Physiological Measurement. 2014; 35(3):351–367. [PubMed: 24480871]

Peters NC, Egen JG, Secundino N, Debrabant A, Kimblin N, Kamhawi S, et al. *in vivo* imaging reveals an essential role for neutrophils in leishmaniasis transmitted by sand flies. Science. 2008; 321(5891):970–974. [PubMed: 18703742]

Proebstl D, Voisin MB, Woodfin A, Whiteford J, D'Acquisto F, Jones GE, et al. Pericytes support neutrophil subendothelial cell crawling and breaching of venular walls *in vivo*. Journal of Experimental Medicine. 2012; 209:1219–1234. [PubMed: 22615129]

Sanz MJ, Johnston B, Issekutz A, Kubes P. Endothelin-1 causes P-selectin-dependent leukocyte rolling and adhesion within rat mesenteric microvessels. American Journal of Physiology. 1999; 277(5):H1823–H1830. Pt 2. [PubMed: 10564136]

Scallan, J.; Huxley, VH.; Korthuis, RJ. In capillary fluid exchange: Regulation, functions, and pathology. Morgan Claypool; San Rafael, CA: 2010.

Shuhendler AJ, Prasad P, Leung M, Rauth AM, Dacosta RS, Wu XY. A novel solid lipid nanoparticle formulation for active targeting to tumor alpha(v) beta(3) integrin receptors reveals cyclic RGD as a double-edged sword. Advanced Healthcare Materials. 2012; 1(5):600–608. [PubMed: 23184795]

Sperandio M, Pickard J, Unnikrishnan S, Acton ST, Ley K. Analysis of leukocyte rolling *in vivo* and *in vitro*. Methods in Enzymology. 2006; 416:346–371.http://dx.doi.org/10.1016/S0076-6879(06)16023-1 [PubMed: 17113878]

Spiller F, Orrico MI, Nascimento DC, Czaikoski PG, Souto FO, Alves-Filho JC, et al. Hydrogen sulfide improves neutrophil migration and survival in sepsis via K+ATP channel activation. American Journal of Respiratory and Critical Care Medicine. 2010; 182(3):360–368. [PubMed: 20339148]

Sriram K, Intaglietta M, Tartakovsky DM. Non-Newtonian flow of blood in arterioles: Consequences for wall shear stress measurements. Microcirculation. 2014; 21(7):628–639. [PubMed: 24703006]

Stark K, Eckart A, Haidari S, Tirniceriu A, Lorenz M, von Bruhl M-L, et al. Capillary and arteriolar pericytes attract innate leukocytes exiting through venules and 'instruct' them with pattern-recognition and motility patterns. Nature Immunology. 2013; 14:41–51. [PubMed: 23179077]

Suematsu M, DeLano FA, Poole D, Engler RL, Miyasaka M, Zweifach BW, et al. Spatial and temporal correlation between leukocyte behavior and cell injury in postischemic rat skeletal muscle microcirculation. Laboratory Investigation. 1994; 70(5):684–695. [PubMed: 7910874]

Suematsu M, Schmid-Schonbein GW, Chavez-Chavez RH, Yee TT, Tamatani T, Miyasaka M, et al. *in vivo* visualization of oxidative changes in microvessels during neutrophil activation. American Journal of Physiology. 1993; 264(3):H881–H891. Pt 2. [PubMed: 8096123]

Sumagin R, Sarelius IH. Intercellular adhesion molecule-1 enrichment near tricellular endothelial junctions is preferentially associated with leukocyte transmigration and signals for reorganization of these junctions to accommodate leukocyte passage. Journal of Immunology. 2010; 184(9): 5242–5252.

Sundd P, Gutierrez E, Koltsova EK, Kuwano Y, Fukuda S, Pospieszalska MK, et al. 'Slings' enable neutrophil rolling at high shear. Nature. 2012; 488(7411):399–403. [PubMed: 22763437]

Sundd P, Pospieszakska MK, Ley K. Neutrophil rolling at high shear: Flat-tening, catch bond behavior, tethers and slings. Molecular Immunology. 2013; 53:59–69. [PubMed: 23141302]

Suzuki H, DeLano FA, Parks DA, Jamshidi N, Granger DN, Ishii H, et al. Xanthine oxidase activity associated with arterial blood pressure in spontaneously hypertensive rats. Proceedings of the National Academy of Sciences of the United States of America. 1998; 95(8):4754–4759. [PubMed: 9539811]

Tallini YN, Brekke JF, Shui B, Doran R, Hwang SM, Nakai J, et al. Propagated endothelial Ca2 + waves and arteriolar dilation *in vivo*: Measurements in Cx40BAC GCaMP2 transgenic mice. Circulation Research. 2007; 101(12):1300–1309. [PubMed: 17932328]

Tyagi N, Givvimani S, Qipshidze N, Kundu S, Kapoor S, Vacek JC, et al. Hydrogen sulfide mitigates matrix metalloproteinase-9 activity and neurovascular per-meability in hyperhomocysteinemic mice. Neurochemistry International. 2010; 56(2):301–307. [PubMed: 19913585]

Voisin MB, Nourshargh S. Neutrophil transmigration: Emergence of an adhesive cascade within venular walls. Journal of Innate Immunity. 2013; 5(4):336–347. [PubMed: 23466407]

Voisin MB, Proebstl D, Nourshargh S. Venular basement membranes ubiquitously express matrix low-expression regions: Characterization in multiple tissues and remodeling during inflammation. American Journal of Pathology. 2010; 176:482–495. [PubMed: 20008148]

Wallace JL, Blackler RW, Chan MV, Da Silva GJ, Elsheikh W, Flannigan KL, et al. Anti-inflammatory and cytoprotective actions of hydrogen sulfide: Translation to therapeutics. Antioxidants & Redox Signaling. 2014

Wang R. The gasotransmitter role of hydrogen sulfide. Antioxidants and Redox Signaling. 2003; 5(4): 493–501. [PubMed: 13678538]

Wang R. Physiological implications of hydrogen sulfide: A whiff exploration that blossomed. Physiological Reviews. 2012; 92(2):791–896. [PubMed: 22535897]

Winterbourn CC. The challenges of using fluorescent probes to detect and quantify specific reactive oxygen species in living cells. Biochimica et Biophysica Acta. 2014; 1840(2):730–738. [PubMed: 23665586]

Woolley JF, Stanicka J, Cotter TG. Recent advances in reactive oxygen species measurement in biological systems. Trends in Biochemical Sciences. 2013; 38(11):556–565. [PubMed: 24120034]

Yuan Y, Chilian WM, Granger HJ, Zawieja DC. Permeability to albumin in isolated coronary venules. American Journal of Physiology. 1993; 265(2):H543–H552. Pt 2. [PubMed: 8368358]

Yuan Y, Mier RA, Chilian WM, Zawieja DC, Granger HJ. Interaction of neutrophils and endothelium in isolated coronary venules and arterioles. American Journal of Physiology. 1995; 268(1):H490–H498. Pt 2. [PubMed: 7840298]

Yusof M, Kamada K, Kalogeris T, Gaskin FS, Korthuis RJ. Hydrogen sulfide triggers late-phase preconditioning in postischemic small intestine by an NO- and p38 MAPK-dependent mechanism. American Journal of Physiology. Heart and Circulatory Physiology. 2009; 296(3):H868–H876. [PubMed: 19168723]

Zanardo RC, Brancaleone V, Distrutti E, Fiorucci S, Cirino G, Wallace JL. Hydrogen sulfide is an endogenous modulator of leukocyte-mediated inflammation. FASEB Journal. 2006; 20(12):2118–2120. [PubMed: 16912151]

Zhang H, Zhi L, Moochhala SM, Moore PK, Bhatia M. Endogenous hydrogen sulfide regulates leukocyte trafficking in cecal ligation and puncture-induced sepsis. Journal of Leukocyte Biology. 2007; 82(4):894–905. [PubMed: 17599903]

Zhu JX, Kalbfleisch M, Yang YX, Bihari R, Lobb I, Davison M, et al. Detrimental effects of prolonged warm renal ischaemia-reperfusion injury are abrogated by supplemental hydrogen sulphide: An analysis using real-time intravital microscopy and polymerase chain reaction. BJU International. 2012; 110(11):E1218–E1227. Pt C. [PubMed: 23046222]

Zuidema MY, Peyton KJ, Fay WP, Durante W, Korthuis RJ. Antecedent hydrogen sulfide elicits an anti-inflammatory phenotype in postischemic murine small intestine: Role of heme oxygenase-1. American Journal of Physiology. Heart and Circulatory Physiology. 2011; 301(3):H888–H894. [PubMed: 21666111]

Zuidema MY, Yang Y, Wang M, Kalogeris T, Liu Y, Meininger CJ, et al. Antecedent hydrogen sulfide elicits an anti-inflammatory phenotype in postischemic murine small intestine: Role of BK channels. American Journal of Physiology. Heart and Circulatory Physiology. 2010; 299(5):H1554–H1567. [PubMed: 20833953]

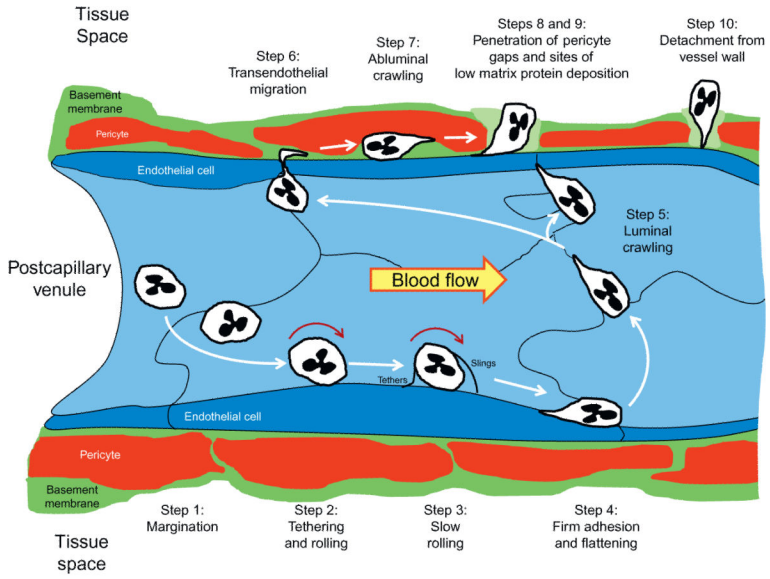

Figure 1.

Neutrophil trafficking to sites of inflammation involves 10 steps. Step 1: *Margination*. As neutrophils exit capillaries and enter the larger diameter postcapillary venular segment of the microcirculation, hydrodynamic forces move granulocytes to the vessel margins (margination). Step 2: *Tethering and rolling*. If appropriate adhesion molecules are expressed on activated endothelial cells and the marginated neutrophil, granulocytes are capture by adhesive interactions that mediate rolling of the leukocyte along the vessel wall. Step 3: *Slow rolling.* The rolling neutrophil monitors its local environment for the presence of activating factors that promote adhesion molecule expression, thereby enabling the leukocyte to further slow its rolling behavior by forming more weak adhesive interactions that are mediated by the selectins. As the cells roll along and interact with P-selectin on the endothelial surface, excess membrane on the surface of neutrophils is pulled out into long nanotubes (microvilli) that form tethers at the rear of the rolling leukocyte. These tethers eventually detach as the cell continues to roll, but do not retract. Instead, they persist and are slung in front of the rolling leukocyte, to interact again with P-selectin. The membranous nanotube is now referred to as a sling, which the neutrophil rolls over to again be retarded in its movement down the vessel wall as the sling transitions to a tethering function. Step 4: *Firm or stationary adhesion*. By establishing strong adhesive interactions mediated by integrin-dependent interactions with endothelial ICAM-1 that are upregulated by chemokines, the slowly rolling leukocyte progresses to firm adhesion. Step 5: *Luminal crawling.* Integrin-ICAM-1-dependent adhesion activates intracellular signaling pathways that induce cytoskeletal changes and polarization of the cell that lead to luminal motility. The crawling neutrophils move along interendothelial junctions in search of preferred routes for diapedesis and are often observed moving against the direction of flow in this exploration. Step 6: *Transendothelial cell migration*. Neutrophils cross the endothelial cell barrier by traversing interendothelial junctions at preferential sites that overlie areas in the basement membrane that exhibit low matrix protein deposition. Occasionally, these inflammatory phagocytes cross the endothelial barrier by moving through cells in a transcellular route. Step 7: *Abluminal crawling.* Once through the endothelium, the

diapedesing neutrophils crawl abluminally along pericyte processes, interacting with basement membrane structures at the same time. Steps 8 and 9: Penetration of pericyte gaps and regions of low matrix protein expression in the basement membrane. Abluminally crawling neutrophils breach the pericyte layer where gaps between these cells exist, which coincide with regions of low matrix protein deposition (depicted as a lighter shade of green) in the basement membrane. These steps occur more or less simultaneously and use different adhesion molecules to propel the leukocyte through these barriers. Step 10: *Detachment from the vessel Wall*. The last step in the process requires detachment of the migrating neutrophil from components of the vessel wall, which involves release of pseudopodial extensions from their sites of attachment to basement membrane components and adhesion receptors on pericytes and endothelial cells. Once this is achieved, the leukocyte follows directional cues provided by a chemotactic gradient and migrates through the tissue space towards inflammatory foci. *Modified from* Voisin and Nourshargh (2013).

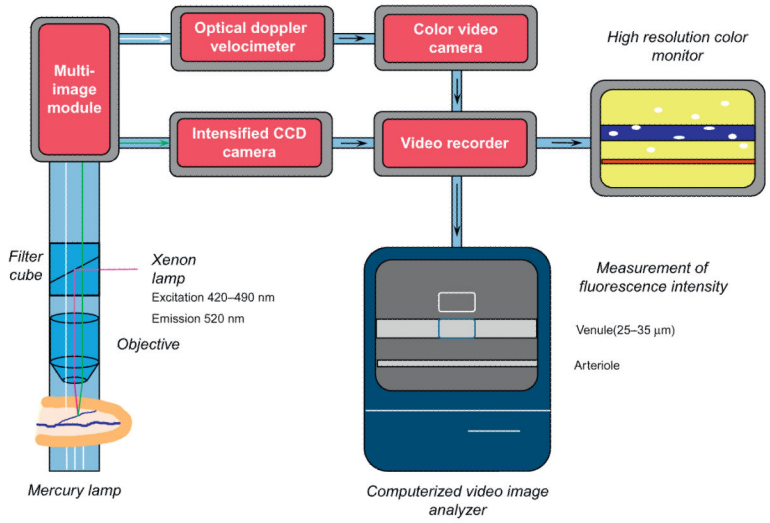

Figure 2.

Graphical representation of components required for intravital microscopic observation of the living microcirculation by trans- or epi-illumination. For transillumination, light from a mercury light source is directed through exteriorized thin (<100 mm) tissues to a salt water immersion microscope objective that focuses the collected image onto a color video camera. Images from the camera are recorded by a DVD recorder and presented on a color television monitor. An optical Doppler velocimeter is incorporated into the light path between the microscope objective and video camera to monitor erythrocyte velocity. Computerized fluorescence intravital microscopy can also be incorporated into this system to quantify venular protein leakage, chemokine or adhesion molecule expression, or oxidant production. Using epifluorescence microscopy, light from a xenon source directed to the tissue under observation via a filter cube, which excites the fluorochrome of interest, causing it to emit light that is collected via the objective and directed to an intensified CCD camera, captured onto a computer (or to videotape or video disc by use of a video or digital video recorder, respectively) for computerized image analysis of fluorescence intensity. A multi-image module directs light to either the color video camera or the CCD camera. Vessel diameter is measured using a videocaliper (not shown) and the numbers of rolling and adherent leukocytes, leukocyte rolling velocity, and mean red cell velocity a quantified during off-line analysis of the collected images. Not shown for simplicity is the animal whose tissues are being observed.

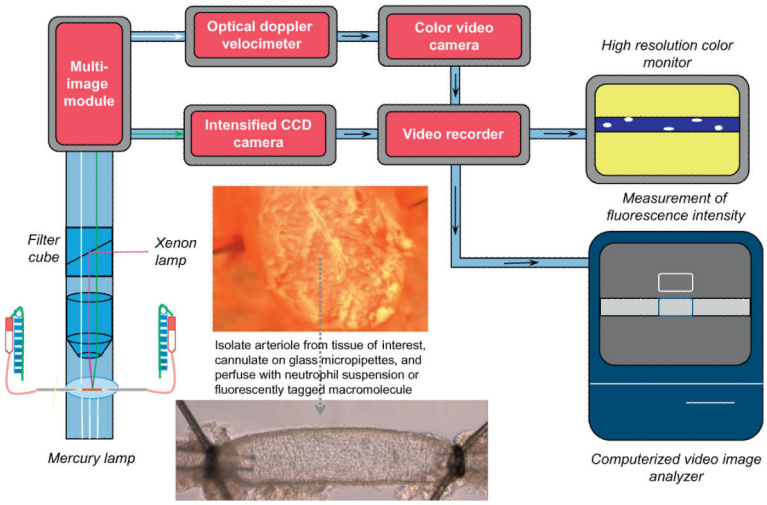

Figure 3.

Schematic representation of essential components for assessment of neutrophil interactions and venular permeability isolated, perfused single postcapillary venules using *ex vivo* microscopy. This approach uses the same components as shown in Fig. 2 for intravital microscopy. The major difference is that an isolated vessel perfusion chamber takes the place of the viewing pedestal animal board. For this preparation, a postcapillary venule is isolated from the tissue of interest, cannulated on glass micro-pipettes and perfused with neutrophils or fluorescently tagged macromolecules. The height of the perfusion reservoirs can be adjusted in equal and opposite directions by use of a pulley system to alter perfusion pressure and flow without altering midpoint pressure in the vessel. Neutrophil–endothelial cell adhesive interactions and venular permeability are determined as described in the text.

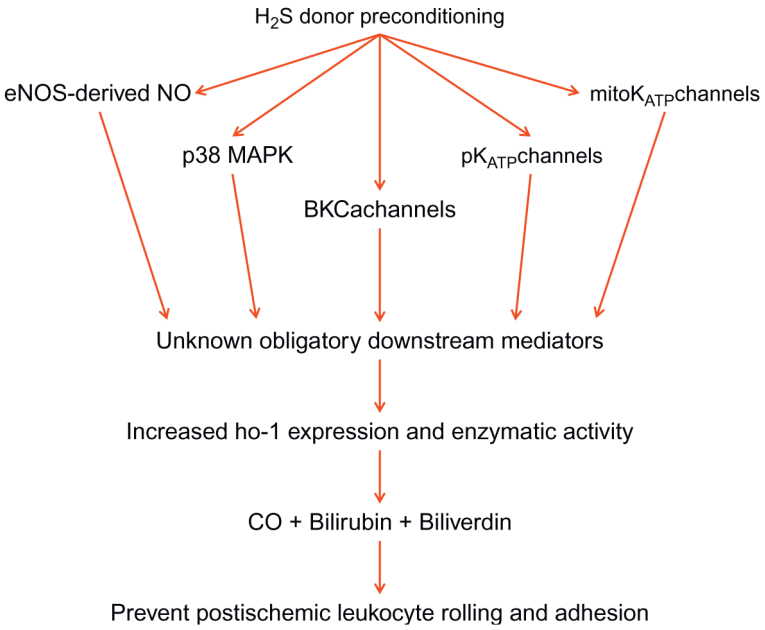

Figure 4.

Signaling mechanisms invoked by antecedent preconditioning with H_2S donors 24 h prior to ischemia/reperfusion. Entrance into a protected state that limits postischemic leukocyte/endothelial cell adhesive interacts is triggered by an eNOS-derived NO-, p38 MAPK-, BKCa- and K_{ATP}-channel-dependent mechanism that is activated during the first hour after H_2S donor administration. These triggering events activate as yet unknown obligatory downstream signaling mediators to promote increased expression and activity of heme oxygenase-1 (HO-1) between 8 and 24 h later. The enzymatic activity of HO-1 generates the anti-adhesive gasotransmitter carbon monoxide (CO) as well as the powerful antioxidants bilirubin and secondarily derived biliverdin, which act in concert to prevent postischemic leukocyte trafficking and neutrophil-dependent parenchymal cell injury.